Diagnostics of premixed burner flame with the superposition of dielectric barrier discharge

Koichi Sasaki

Division of Quantum Science and Engineering, Hokkaido University
Kita 13, Nishi 8, Kita-ku, Sapporo 060-8628, Japan

We examined premixed burner flame with the superposition of dielectric barrier discharge (DBD) to identify the key species in plasma-assisted combustion. The density of OH, which is widely considered to be most important in plasma-assisted combustion, did not respond to the pulsed production of high-energy electrons in DBD. On the other hand, the density of atomic oxygen showed sensitive response to the pulsed high-energy electrons in the transition region between unburned gas and the reaction zone. This suggests that additional atomic oxygen in the transition region, which is produced by electron impact processes, works as the key species in the plasma-assisted flame.

1. Introduction

Recently, plasma-assisted combustion has attracted scientific and industrial interests because of its potential in improving speedy-flow combustion, stabilizing lean flame, and enhancing burning velocity. Although it is believed that the modified combustion is caused by the effect of high-energy electrons in nonequilibrium plasma, the specific discussion of the effect of high-energy electrons on the enhancement of combustion reactions is still insufficient. The principal issues to be understood in plasma-assisted combustion are to identify the key species, key reactions, and concrete roles of high-energy electrons.

In this work, we adopted laser-aided diagnostics to premixed burner flame with the superposition of dielectric barrier discharge (DBD). DBD produces high-energy electrons in a pulsed mode automatically. Our idea is that the species which has the density with sensitive response to pulsed high-energy electrons has a close relationship to the origin of the modified combustion of plasma-assisted flame [1]. We measured the temporal variations of the density of OH($X^2\Pi$), the rotational temperature of OH($X^2\Pi$), the gas temperature, the optical emission intensity of Ar, the optical emission intensity of OH (or the density of OH($A^2\Sigma^+$)), the rotational temperature of OH($A^2\Sigma^+$), and the density of atomic oxygen at the ground state. The experimental result suggests the importance of atomic oxygen in plasma-assisted combustion.

2. Experiment

We employed a premixed burner with $CH_4/O_2/Ar$ mixture. The flow rates of CH_4, O_2, and Ar were adjusted to 0.38, 1.0, and 5.6 slm, respectively, using mass flow controllers. The length of the flame was approximately 85 mm. The side of the slender flame was partly covered with a quartz tube. The distance between the bottom side of the quartz tube and the top of the burner nozzle was 13 mm, and the length of the quartz tube was 65 mm. An aluminum electrode was attached on the outside of the quartz tube. The distance between the bottom side of the electrode and the top of the burner nozzle was 25 mm, and the axial length of the electrode was 10 mm. A high-voltage power supply with a rectangular waveform was connected to the aluminum electrode, while the burner nozzle worked as the ground electrode. We thus obtained asymmetric DBD inside the quartz tube.

We adopted conventional optical emission spectroscopy for measuring the optical emission spectra of Ar and OH. The temporal variation of the optical emission spectra was obtained by changing the delay time between the current pulse and the trigger for the gate opening of an ICCD camera which was attached to a spectrograph. The rotational temperature of OH($A^2\Sigma^+$) was evaluated by analysing the optical emission spectrum of OH. The radial distribution of the gas temperature was evaluated by laser Rayleigh scattering. An OPO laser beam at a wavelength of 250 nm was focused using a lens, and was injected into the flame. The image of the Rayleigh-scattered laser light was captured using an ICCD camera via an interference filter. The gas temperature was deduced by comparing the intensity of the scattered laser light in the flame with that in ambient air at room temperature. The temporal variation of the gas temperature was obtained by changing the delay time between the current pulse and the laser oscillation. The densities of OH($X^2\Pi$) and ground-state atomic oxygen were measured by laser-induced fluorescence (LIF). We obtained the

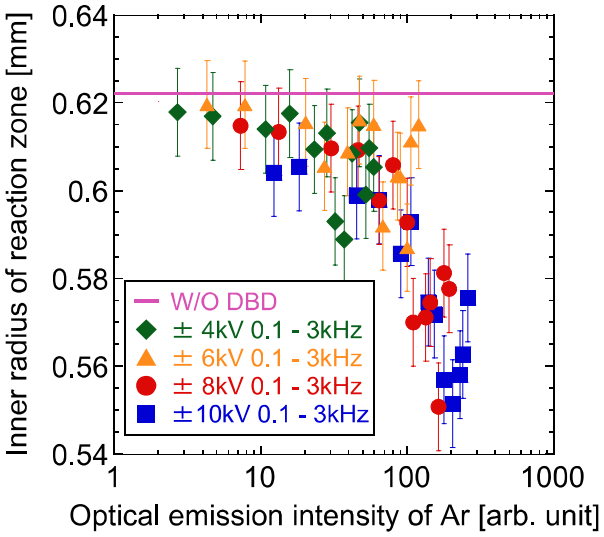

Fig. 1 Relationship between the radius of the reaction zone and the optical emission intensity of Ar.

two dimensional distribution of the OH($X^2\Pi$) density by adopting planar LIF. The distribution of the rotational temperature of OH($X^2\Pi$) was deduced from the LIF intensities observed at various laser wavelengths corresponding to the excitations from various rotational states. The O atom density was measured by two-photon absorption LIF. In this case, we employed a focused laser beam, and we obtained one-dimensional (radial) distribution of the O atom density along the path of the laser beam. The temporal variation of the OH($X^2\Pi$) and O densities were obtained by changing the delay time between the current pulse and the laser oscillation.

3. Results

3.1. Enhancement of burning velocity

Figure 1 shows the relationship between the optical emission intensity of Ar and the inner radius of the region with the optical emission intensity of OH [2]. Note that this result was obtained by time-integrated measurements over the cycles of the discharge voltage. The horizontal line shows the inner radius of the region with optical emission intensity of OH in the absence of DBD. The optical emission intensity of OH represents the location of the reaction zone. According to the fundamental of combustion science, the shape of the reaction zone is determined by the balance between the gas flow speed and the burning velocity, and the shrinkage of the radius of the reaction zone indicates the increase in the burning velocity. On the other hand, the optical emission of Ar was observed only in the DBD-assisted flame, and we estimated the amount of high-energy electrons from the optical emission intensity of Ar. As shown in Fig. 1, we observed a unique relationship between the amount of high-energy electrons and the enhancement of the burning velocity, even though the optical emission intensity of Ar was varied by various ways. The experimental result shown in Fig. 1 clearly indicates that the amount of high-energy electrons is the most important parameter in plasma-assisted combustion. The next step is to find the chemical species which has direct response to high-energy electrons.

3.2. Temporal variations of various quantities

Figure 2 shows the temporal variations of various quantities in a cycle of DBD. The waveforms of the discharge voltage and the discharge current are shown in Fig. 2(a). The waveform of the discharge current was obtained by averaging 512 cycles on a digital oscilloscope. The current pulse in a single cycle had a duration of approximately 5 μs. However, since the jitter in the discharge current was unavoidable, the averaged current waveforms had longer durations, as shown in the figure.

The temporal variation in the optical emission intensity of Ar is shown in Fig. 2(b). It is clearly shown in Fig. 2(b) that the optical emission intensity of Ar is observed simultaneously with the current pulses. In addition, the optical emission intensity of Ar in the falling phase of the discharge voltage is higher than that in the rising phase.

The temporal variation of the OH($X^2\Pi$) density is shown in Fig. 2(c). The measurement position is in the reaction zone of the flame. The vertical axis of Fig. 2(c) is normalized by the OH($X^2\Pi$) density at the same position in the absence of DBD. As shown in the figure, the OH($X^2\Pi$) density in the presence of DBD was slightly higher than that in the absence of DBD in almost all the discharge phases. However, we never observed pulsed increases in the OH($X^2\Pi$) density simultaneously with the current pulses.

The temporal variation in the optical emission intensity of OH, or the density of OH($A^2\Sigma^+$), is shown in Fig. 2(d). The vertical axis is normalized by the optical emission intensity of OH in the absence of DBD. It is clear from the figure that the OH($A^2\Sigma^+$) density increased simultaneously with the current pulses. In addition, it is noted that a higher OH($A^2\Sigma^+$) density was observed when a lower optical emission intensity of Ar was observed.

Figure 2(e) shows the temporal variation in the gas temperature, and Fig. 2(f) shows the rotational temperatures of OH($X^2\Pi$) and OH($A^2\Sigma^+$). The

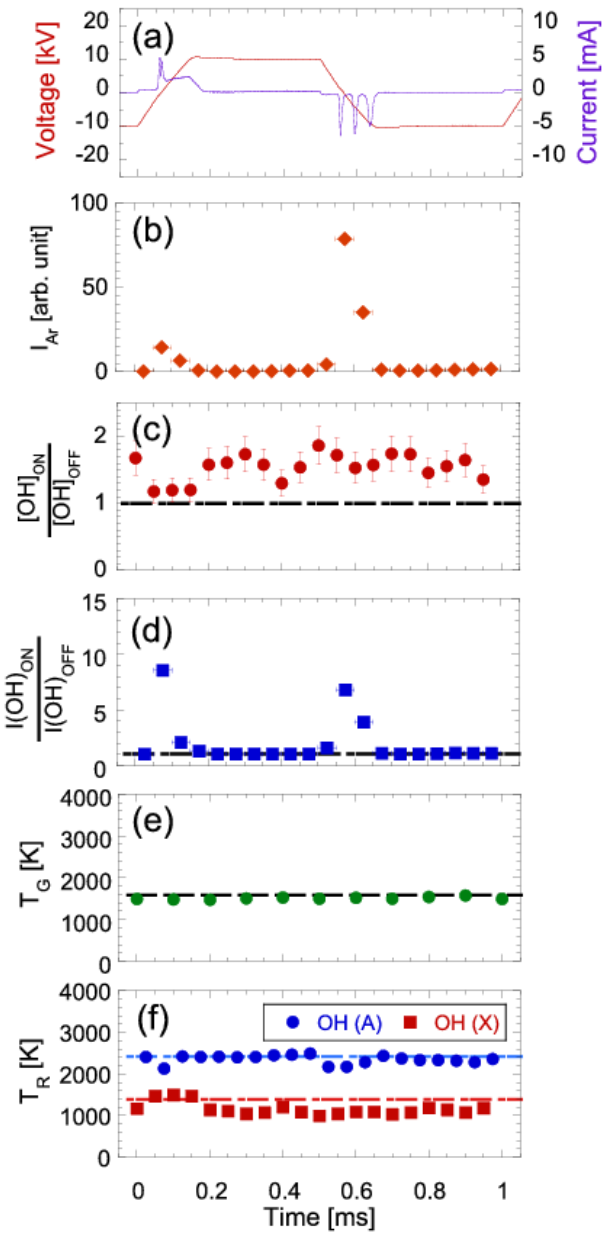

Fig. 2 Temporal variations in various quantities in a cycle of DBD: (a) waveforms of the discharge voltage and discharge current, (b) optical emission intensity of Ar, (c) density of $OH(X^2\Pi)$, (d) optical emission intensity of OH, (e) gas temperature, and (f) rotational temperatures of $OH(X^2\Pi)$ and $OH(A^2\Sigma^+)$.

horizontal lines show the temperatures in the absence of DBD. As shown in Fig. 2(e), we observed no gas heating in the presence of DBD, and the gas temperature was constant in the discharge cycle. We observed the decrease in the rotational temperature of $OH(X^2\Pi)$ in the presence of DBD, but the decrease in the rotational temperature of $OH(X^2\Pi)$ was not pulsed. It should be emphasized here that we observed pulsed decreases in the rotational temperature of $OH(A^2\Sigma^+)$ simultaneously with the current pulses.

Figure 3 shows the temporal variation of the O atom density. The vertical axis is normalized by the O density in the absence of DBD. As shown in Fig. 3(a), the O atom density responded to the current pulses at a radial position of 1 mm. According to the radial distribution of the gas temperature, this radial position corresponded to the transition region (preheating zone) between unburned gas and the reaction zone. On the other hand, at radial positions of 1.5 and 2 mm, the temporal variation of the O density was not remarkable.

4. Discussion

We observed a higher $OH(X^2\Pi)$ density in the presence of DBD, as shown in Fig. 2(c). It is certain that the increase in the $OH(X^2\Pi)$ density is attributed to high-energy electrons provided by DBD. The lower rotational temperature of $OH(X^2\Pi)$ suggests a change in their production pathways in the presence of DBD. However, it is important to note that the increase in the $OH(X^2\Pi)$ density is not a direct effect of electron impact processes, since we never observed pulsed increases in the $OH(X^2\Pi)$ density simultaneously with the current pulses. It is considered that the stationary increase in the $OH(X^2\Pi)$ density is "not the origin" but is "a result" of improved combustion reactions in the plasma-assisted flame.

According to Fig. 3(b), a larger amount of high-energy electrons is available at the falling phase of the discharge voltage. In contrast, a higher optical emission intensity of OH was observed at the rising phase of the discharge voltage, as shown in Fig. 2(d). This result indicates that the optical emission intensities of OH simultaneously with the current pulses are not governed by electron impact excitation, and that chemiluminescence is remarkable in the optical emission of OH even in the DBD-assisted flame. According to the experimental result shown in Fig. 2(d), the chemical production process of $OH(A^2\Sigma^+)$ becomes efficient only when high-energy electrons are available. In addition, according to Fig. 2(f), $OH(A^2\Sigma^+)$ produced simultaneously with the current pulse has a lower rotational temperature. These observations give us a useful hint for estimating the key species in plasma-assisted combustion.

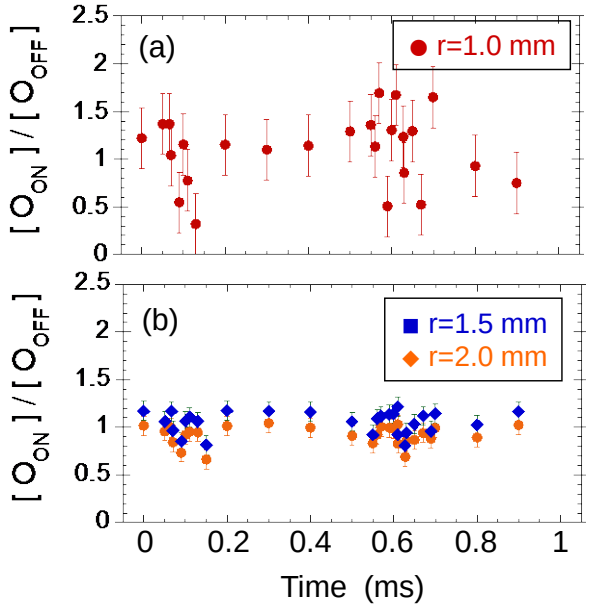

Fig. 3 Temporal variations of the densities of atomic oxygen observed at a radial position of (a) 1.0 mm and (b) 1.5 and 2.0 mm.

Becker and coworkers have pointed out that there are three processes which produce $OH(A^2\Sigma^+)$ in combustion chemistry [3,4]. According to Becker and coworkers, $H+O+M \rightarrow OH(A^2\Sigma^+)+M$ and $CH+O_2 \rightarrow OH(A^2\Sigma^+)+CO$ produce $OH(A^2\Sigma^+)$ with a high rotational temperature ("hot $OH(A^2\Sigma^+)$"), while $CHO+O \rightarrow OH(A^2\Sigma^+)+CO$ produces $OH(A^2\Sigma^+)$ with a low rotational temperature ("cold $OH(A^2\Sigma^+)$"). Comparing the results of Becker and coworkers with our experimental observations, it is suggested that the production of $OH(A^2\Sigma^+)$ via $CHO+O \rightarrow OH(A^2\Sigma^+)+CO$ becomes efficient in the presence of high-energy electrons. In other words, it can be speculated that the decreases in the rotational temperature of $OH(A^2\Sigma^+)$ simultaneously with the current pulses are caused by the production of atomic oxygen by electron impact dissociation of O_2. Since electron impact dissociation decomposes CHO, the optical emission intensity of OH in the falling phase of the discharge voltage is lower than that in the rising phase.

The sensitive response of the density of atomic oxygen to the current pulses has been confirmed as shown in Fig. 3(a). However, as shown in Fig. 3(b), the response of the O density to the current pulses was not observed in the reaction zone. This means that the production of atomic oxygen is governed by combustion reactions in the reaction zone, even when high-energy electrons are provided. On the other hand, in the transition region between unburned gas and the reaction zone, the increase in the O density at the timing of the current pulses is remarkable. In addition, the increases in the O density is followed by the rapid decreases, suggesting the consumption of additional atomic oxygen by combustion reactions since it works a reactive oxidizer.

5. Conclusions

In this work, we examined the temporal variations of in the density of $OH(X^2\Pi)$, the rotational temperature of $OH(X^2\Pi)$, the gas temperature, the optical emission intensity of Ar, the density of $OH(A^2\Sigma^+)$, the rotational temperature of $OH(A^2\Sigma^+)$, and the density of atomic oxygen in DBD-assisted premixed burner flame. The experimental results suggest that the production of atomic oxygen in the transition region between unburned gas and the reaction zone is the origin of improved combustion in the plasma-assisted flame.

[1] K. Zaima and K. Sasaki, Jpn. J. Appl. Phys. **53**, 110309 (2014)

[2] K. Zaima and K. Sasaki, Jpn. J. Appl. Phys. **53**, 066202 (2014)

[3] K. H. Becker and D. Kley, Chem. Phys. Lett. **4**, 62 (1969)

[4] K. H. Becker, D. Kley, and R. J. Norstrom, *Molecular Luminescence*, Ed, E. C. Lim (Benjamin, Inc., New York, 1969) p. 509.